

# Signal Transmission through the Dark-adapted Retina of the Toad (*Bufo marinus*)

## *Gain, Convergence, and Signal/Noise*

DAVID R. COPENHAGEN, SIMO HEMILÄ, and TOM REUTER

From the Departments of Ophthalmology and Physiology, University of California School of Medicine, San Francisco, California 94143-0730; the Laboratory of Physics, Helsinki University of Technology, SF-02150 Espoo, Finland; and the Department of Zoology, University of Helsinki, SF-00100 Helsinki, Finland

**ABSTRACT** Responses to light were recorded from rods, horizontal cells, and ganglion cells in dark-adapted toad eyecups. Sensitivity was defined as response amplitude per isomerization per rod for dim flashes covering the excitatory receptive field centers. Both sensitivity and spatial summation were found to increase by one order of magnitude between rods and horizontal cells, and by two orders of magnitude between rods and ganglion cells. Recordings from two hyperpolarizing bipolar cells showed a 20 times response increase between rods and bipolars. At absolute threshold for ganglion cells (Copenhagen, D.R., K. Donner, and T. Reuter. 1987. *J. Physiol.* 393:667-680) the dim flashes produce 10-50- $\mu$ V responses in the rods. The cumulative gain exhibited at each subsequent synaptic transfer from the rods to the ganglion cells serves to boost these small amplitude signals to the level required for initiation of action potentials in the ganglion cells. The convergence of rod signals through increasing spatial summation serves to decrease the variation of responses to dim flashes, thereby increasing the signal-to-noise ratio. Thus, at absolute threshold for ganglion cells, the convergence typically increases the maximal signal-to-noise ratio from 0.6 in rods to 4.6 in ganglion cells.

### INTRODUCTION

The most sensitive retinal ganglion cells in dark-adapted toad and frog retinas can respond to flashes that isomerize only 10-20 rhodopsin molecules within their receptive fields, which encompass on the order of  $10^3$  rods (Donner, 1981, 1989; Reuter et al., 1986; Copenhagen et al., 1987). At these low light levels, it is obvious, because of the statistics of quantal fluctuations, that the number of isomerizations per flash must vary considerably when the retina is exposed to a series of "identical"

Address reprint requests to Dr. Tom Reuter, Department of Zoology, University of Helsinki, Arkadiankatu 7, SF-00100 Helsinki, Finland.

threshold flashes. This variability is here termed photon noise. Sometimes it is possible to observe a spike response variation which, to a significant degree, is caused by the photon noise (Aho et al., 1987).

Besides the photon noise there is another inevitable noise source that also reduces the reliability (signal-to-noise ratio, SNR) of all neuronal responses in a dark-adapted toad retina: even in complete darkness *Bufo marinus* rods produce spontaneous events that are randomly distributed in time and indistinguishable from photon-induced isomerizations (Baylor et al., 1980). This "dark noise" degrades the statistical significance of a weak flash of light in the same way as the rain of photons in a background of real light does.

An upper limit to the signal-to-noise ratio of a rod or ganglion cell response can be computed by considering the Poisson variation of the numbers of stimulus isomerizations and dark rod events (and possible isomerizations originating from background lights). For Poisson distributed numbers the standard deviation equals the square root of the mean. The upper limit to the response reliability is then given by the equation:

$$\text{SNR} = E_s / (E_s + E_b + E_d)^{0.5} \quad (1)$$

where  $E_s$  is the mean number of isomerizations (within the receptive field of the cell) produced by the flash stimulus,  $E_d$  is the mean number of dark isomerization-like events interacting with the stimulus (i.e., occurring within the receptive field and integration time of the cell), and  $E_b$  is the mean number of background-induced isomerizations interacting with the stimulus ( $E_b = 0$  for darkness) (Barlow, 1964; Copenhagen et al., 1987). From Eq. 1 it follows that the (maximum) signal-to-noise ratios of responses to a given diffuse flash increase with the square root of the receptive field size, i.e., the square root of the number of contributing rods.

In this and the accompanying paper (Donner et al., 1990) we have approached the signal-to-noise aspect of cellular responses at two different levels: (a) we have measured the spatial and temporal summation characteristics of rods, horizontal cells, and ganglion cells, and then determined maximum response reliabilities by applying Eq. 1; (b) we have compared such calculated signal-to-noise ratios with physiologically observed noise in the form of membrane potential fluctuations in rods and horizontal cells, and (extracellularly recorded) maintained spike activity in ganglion cells.

In this paper we concentrate on the effective increase in spatial summation occurring in the signal transmission between rods and ganglion cells, and further we will describe the voltage amplification observed in the retina. In the following paper we investigate how the rods and horizontal cells in the distal retina, and the ganglion cells in the proximal, adjust to the noise and the saturation risk produced by weak and modest backgrounds of light. There we thus see how steady background lights affect the signal transfer through the retina.

Both studies are based on intracellular recordings from rods and horizontal cells, and extracellular recordings from ganglion cells. A few intracellular bipolar and ganglion cell recordings give us direct but rough information about voltage amplification. In several instances we refer to results obtained in a previous study based on extracellular ganglion cell recordings (Copenhagen et al., 1987). All experiments

have been carried out in exactly the same type of eyecup preparation. By the symbol  $Rh^*$  we denote one photoisomerization per rod.

#### METHODS

The preparation of the eyecup and its maintenance during experiments has been described in a previous study (Copenhagen et al., 1987). The same study presented the methods for light stimulation and calibration of light intensities, and the basis for their expression in the form of numbers of isomerizations per rod per second ( $Rh^*s^{-1}$ ). Stimuli having an intensity  $1 Rh^*s^{-1}$  were produced by a  $1.6 \mu\text{lux}$  beam of 500 nm light entering the retina in a direction parallel to the rod outer segments. The flash stimuli were 13.5 ms in duration and their strength was expressed as the numbers of isomerizations per rod.

##### *Intracellular Recording*

Microelectrodes were drawn on a Brown-Flaming airblast electrode puller (Sutter Instruments Co., San Francisco, CA) and back-filled with a 2 M potassium acetate. Resistances, as measured in the vitreous with a DC current pulse, ranged from 500 to 900 M $\Omega$ . The electrodes were advanced (using a high speed stepper motor, Brown and Flaming, 1977) into the retina from the vitreal side at an angle of  $\sim 35^\circ$  from the perpendicular. Cell penetration was facilitated by "buzzing" the microelectrode with increased capacitance compensation. Cellular potentials were DC-amplified, displayed on a storage oscilloscope, and recorded on magnetic tape (Racal Recorders, Inc., Sarasota, FL).

##### *Histology*

The Lucifer yellow staining of electrophysiologically characterized retinal neurons, and the subsequent histological procedures, were carried out as described by Ashmore and Copenhagen (1983). The stained cells were inspected first in whole-mounts and then in radially cut sections. The relative numbers of cells in different retinal layers were determined from vertical sections.

##### *Electrophysiological and Histological Cell Identification*

Intracellular recordings were made from various classes of nonspiking and spiking cells. The relative and absolute sensitivities to dim 500 and 600 nm stimuli showed that we recorded neither from cones nor from the blue-sensitive green rods. We discriminated between rods and horizontal cells, which produce qualitatively similar responses to weak stimuli, by mapping the receptive fields of these cells, by noting the relative retinal depths of the microelectrode impalements, and by observing the response to bright flashes ( $1,300 Rh^*$  or more). Rod responses to bright flashes exhibited a fast transient hyperpolarization, a "nose," followed by a plateau phase (Brown and Pinto, 1974). Horizontal cell responses lacked the fast transient nose (Belgum and Copenhagen, 1988).

Under stimulus conditions that favored cone inputs (e.g., wavelengths  $> 580$  nm), a transient hyperpolarization, a "hump," could be observed at the peak of horizontal cell flash responses. The duration of this hump, at 50% of its maximum, was typically  $\sim 0.8$  s ( $10^4 Rh^*$ , 600 nm diffuse flash), while the corresponding duration of the rod "nose" was  $\sim 0.2$  s. This cone-driven hump exhibited a larger receptive field than the rod-driven part of the horizontal cell response. The results covered in this study are restricted to the rod-driven component of the horizontal cell response.

The above physiological identifications agreed very well with the combined histological and physiological cell identifications presented by Fain (1975, 1976) and Hassin and Witkovsky (1983). They were further confirmed by a few Lucifer yellow injections; one rod and three

horizontal cells were both physiologically characterized and histologically identified. Fig. 1 shows the rod and two of the horizontal cells, together with the responses of the rod and one of the horizontal cells, to bright flashes. The horizontal cells had relatively small dendritic trees (diameter,  $\sim 40 \mu\text{m}$ ), and a long axon with small ascending processes and a bifurcated ending (see drawing in Fig. 1). One of these horizontal cells was recovered in a vertical section, and both the dendritic endings and the short processes ascending from the axon were seen to reach the receptor terminals. The injected horizontal cells resembled the "inner horizontal cells" described in the frog retina (Ramón y Cajal, 1972; Ogden et al., 1984).

Useful recordings were obtained from only two (hyperpolarizing) bipolar cells. One of them was identified by Lucifer Yellow injection. These cells had faster flash responses than the rods and horizontal cells and a pronounced high-frequency voltage noise in darkness that was suppressed during light-evoked hyperpolarizations. Two spiking cells had been injected

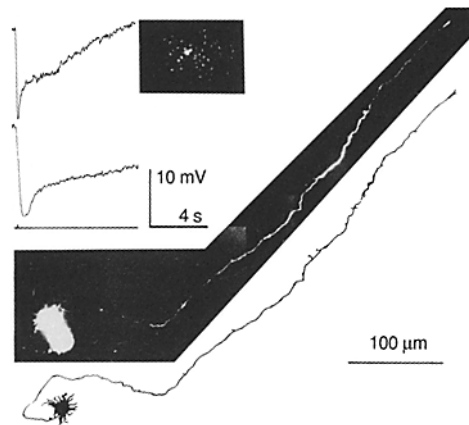


FIGURE 1. Lucifer yellow-stained rod and horizontal cell. Lucifer dye was injected intracellularly into two horizontal cells and one rod in the same retina. The two horizontal cells were separately injected during two penetrations along the same path. Photographs were taken of the stained cells in the isolated, flat-mounted retina which was viewed from the receptor side. The drawing just below the photograph traces the cell body and axon process of one of the dye-filled horizontal cells. Cross sections of the same cells in plastic-embedded sections revealed that the

small twig-like projections along the axon appeared to make contact with photoreceptor terminals. The upper photograph is a similar flat-mounted view of a rod. The photograph was taken with combined epi (fluorescent excitation) and transmitted illumination. The bright spot in the center is the dye-filled rod; the surrounding spots are neighboring unfilled rods seen in transmitted illumination. In the upper left, responses are shown from these same dye-injected cells. The light stimulus was a  $750 \mu\text{m}$  diam, 500 nm light, producing  $10^4 \text{ Rh}^*$  per 13.5-ms flash.

with Lucifer; one of them turned out to be an amacrine cell, the other a ganglion cell that had a well-stained axon reaching the optic disc.

Except for the bipolar cell, the Lucifer-injected cells were used just for cell-type identification; the recordings were not stable and noise free enough for quantitative investigations.

The mean rod membrane potential in darkness, determined from the voltage change observed upon withdrawing the electrode from the cell, was  $-43 \text{ mV}$  (range, 39–48;  $n = 32$ ), and the mean horizontal cell membrane potential was  $-30 \text{ mV}$  (range, 22–37,  $n = 9$ ), while the three spiking cells from which we obtained stable intracellular recordings had resting potentials between  $-50$  and  $-65 \text{ mV}$ .

#### *Terminology and Definitions*

*Flash sensitivity,  $S_F$ .* The peak amplitude of a flash-evoked response per  $\text{Rh}^*$  ( $\text{mV}/\text{Rh}^*$ ), as obtained with stimulus fields large enough to cover the whole summation area of the rod

or horizontal cell under study. This would be the maximum sensitivity since the eyes were fully dark-adapted, and the amplitudes were determined in the linear part of the intensity-response function. When relating the sensitivity of ganglion cells to the sensitivities of rods and horizontal cells, we ignored the spikes and used the amplitude of the slow flash-evoked depolarization per  $Rh^*$  ( $mV/Rh^*$ ), as obtained with responses to very dim flashes covering the excitatory receptive field center. When plotting the intensity-response function of a ganglion cell in Fig. 3 (see below) we use the number of spikes as a measure of relative response strength. In the accompanying paper (Donner et al., 1990), in which all ganglion cell results are based on extracellular recording, the flash sensitivity is defined as the reciprocal of the flash intensity needed for a threshold spike response ( $1/Rh^*$ ).

*Voltage gain of signal transfer.* The ratio of the flash sensitivities of two classes of neuron, e.g.,  $S_F$  (horizontal cell)/ $S_F$  (rod). This use of the term voltage gain is consistent with that of Ashmore and Falk (1980), Schnapf and Copenhagen (1982), and Capovilla et al. (1987).

*Spatial summation.* When discussing the spatial summation of ganglion cells we refer to the summation within the excitatory receptive field center.

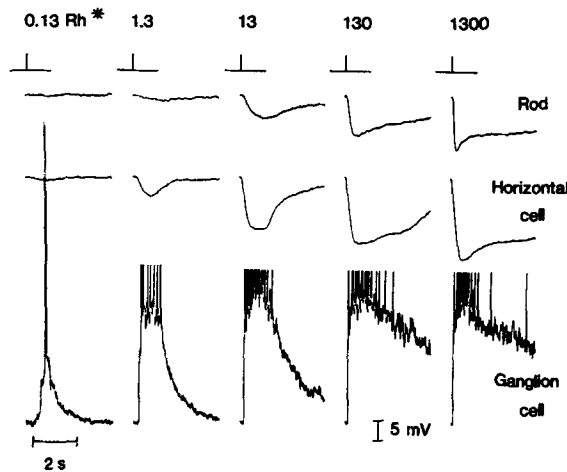


FIGURE 2. Comparison of rod, horizontal cell, and spiking cell (presumed ganglion cell) responses to the same five flash intensities (shown along the upper row). Flash duration, 13.5 ms. The stimulus spots were blue-green (500 nm) and 750  $\mu m$  in diameter; flash duration was 13.5 ms. All responses are shown at the same amplification (bar, 5 mV) and duration (4 s). The amplitude of the entire action potential is shown in the first column. For clarity, the spikes were truncated in the responses to higher flash intensities.

## RESULTS

The intracellular voltage responses from a rod, a horizontal cell, and a ganglion cell are shown in Fig. 2 for flash intensities spanning a range of  $10^4$ . A comparison of these flash responses qualitatively illustrates two aspects of signal processing that are the subjects of this study: the amplification of light responses through the retina, and the increase in the signal-to-noise ratio by which the ganglion cell responds in a robust fashion to flash intensities at which the rod responses are imperceptible. The dimmest flash ( $0.13 Rh^*$ ) depolarized the ganglion cell by 20 mV, which was sufficient to evoke action potentials while no rod response exceeding the level of random potential fluctuations was seen. It is obvious that this increase in signal-to-noise ratio is due to the fact that the signal amplitude grows more than the noise. Our

desire to further elucidate and quantify this signal amplification and signal detection was the main impetus for this study.

### Intensity-Response Functions and Voltage Gain

Complete intensity-response functions were determined for 17 rods and 5 horizontal cells. The most sensitive of them are shown in Fig. 3. For illustrating the intensity-response function of a "typical" ganglion cell we used the spiking cell shown in Fig. 2; these intracellularly recorded spike responses had a threshold (0.025 Rh\*) and an intensity-spike number function that was typical of a large number of extracellularly recorded ganglion cells in dark-adapted *Bufo marinus* retinas (Copenhagen et al., 1987; the average threshold of 19 cells was 0.029 Rh\*). The amplitudes of

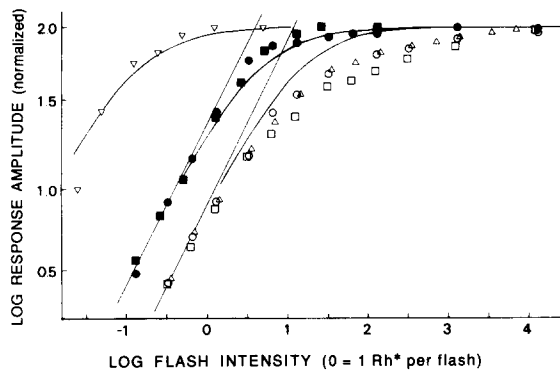


FIGURE 3. Intensity vs. peak response functions for one representative ganglion cell (open inverted triangles), two horizontal cells (filled symbols), and three rods (open circles, triangles, and squares). Log  $I$  is scaled in Rh\*/flash (13.5 ms, 520 or 750  $\mu$ m diam, 500 nm) where 0 = 1 Rh\*/flash. The ordinate, log  $V$  is normalized to  $V_{\max}$  (by multiplying  $V/V_{\max}$  by 100) for each rod and horizontal cell ( $V_{\max}$ : ● = 18.0 mV,

■ = 15.5 mV, ○ = 19.0 mV, △ = 15.0 mV, □ = 19.5 mV). The sensitivities of the three rods were 1.1, 1.5, and 1.6 mV/Rh\*, and of the two horizontal cells 6.14 and 9.25 mV/Rh\*. The "nose" appearing in rod responses at high intensities is included. Cone-driven "humps" in horizontal cell responses are not included. For the ganglion cell the ordinate signifies normalized number of action potentials within 1.7 s (the integration period of this dark-adapted cell) after the first spike, log  $V = 2.0$  corresponding to 15 spikes. To obtain reliable data in the small-response end of the intensity-response functions we averaged two to five responses at each intensity (this applied to all cell types). Straight lines plot a linear relation between intensity and response amplitude. Curved lines plot the Michaelis relation  $V/V_{\max} = I/(I + I_{0.5})$  where  $V/V_{\max}$  is the fraction of the maximal response,  $I$  is the intensity of the test stimulus (Rh\*) and  $I_{0.5}$  the intensity for a half-maximal response of the assumed Michaelis function.

rod-driven horizontal cell responses went from just detectable to its maximum over stimulus intensities that ranged from 0.1 to 30 Rh\* while the rods produced detectable responses that were graded with intensity from 0.3 to  $10^4$  Rh\*. These curves demonstrate that only the low amplitude responses of the rods are proportionately transmitted to the horizontal cells and ganglion cells. Above log  $I = 1$  (10 Rh\*) the rod responses still increase by a factor of four but that has very little effect on the amplitude of the horizontal cell response. This "clipping" of the rod signal in the transfer to horizontal cells of *B. marinus* has been previously reported (Belgium et al., 1983; Belgium and Copenhagen, 1988). This same clipping is evident at the rod synapse of tiger salamanders (Attwell et al., 1987).

The voltage gain of signal transfer manifests itself at flash intensities where the response amplitudes are linear with intensity. The straight lines in Fig. 3 show the linear regions of the two horizontal cell intensity-response functions (*filled symbols*) and the three rod intensity-response functions (*open symbols*). The intensity-response function for both rods and horizontal cells was linear at intensities below 1 Rh\* ( $0 = 1 \text{ Rh}^*$ ). Interestingly, for both cell types the linearity ends at the same stimulus intensity but at very different normalized response amplitudes; in fact, the linear relationships between the intensity and the amplitudes of the rod and horizontal cell responses break down only just before the saturation of the horizontal cell response. The mean flash sensitivities,  $S_F$ , derived from the slopes of the intensity-response curves to dim flashes, were 0.9 mV/Rh\* for rods (range, 0.7–1.1,  $n = 11$ ) and 6.5 mV/Rh\* for horizontal cells (range, 2.3–9.9,  $n = 7$ ). The cells included in

TABLE I  
*Receptive Field Data for Dark-adapted Rods and Horizontal Cells*

Rods		Horizontal cells			
Cell	Mean length constant	Cell	Mean length constant of flanks of receptive field	Radius of "Gaussian" receptive field	No. of rods in receptive field
	$\mu\text{m}$		$\mu\text{m}$	$\sqrt{2} \sigma, \mu\text{m}$	
1	24	1	33	44	91
2	24	2	27	72	244
3	25	3	31	61	175
4	26	4	50	89	373
5	22	5	61	75	265
6	24	6	44	80	302
7	21	7	45	80	302
8	14				
Mean	22.5		41.6	71.6	250

The number of red rods per micrometer<sup>2</sup> is 0.015 (Copenhagen et al., 1987).

these means were selected from larger sets of units on the basis of the completeness of their characterization (see Donner et al., 1990; Table I).

We obtained no recordings from depolarizing bipolar cells and only two relatively short recordings from hyperpolarizing bipolars. The flash sensitivities of the latter were 19 and 22 mV/Rh\*.

The flash sensitivities obtained from the three spiking cells from which we obtained stable intracellular recordings were 88, 130, and 150 mV/Rh\*. The mean threshold of extracellularly recorded ganglion cell responses was 0.029 Rh\* (range, 0.008–0.062,  $n = 19$ ; Copenhagen et al., 1987). On the assumption that a 5–10 mV depolarization was required for these threshold responses, the corresponding flash sensitivities would be 80–1,250 mV/Rh\*. Observe that all electrophysiological recordings favor large ganglion cells over small ones. Thus the above numbers hardly are representative for all ganglion cells.

*Receptive Fields of Rods and Horizontal Cells*

For the purpose of determining signal-to-noise ratios we first measured the receptive field profile of each class of retinal neuron. Then we tried to “translate” these profiles to imaginary groups of equally sensitive rods, groups which (considering the limits set by Eq. 1) would respond to diffuse stimuli with the same (maximum) signal-to-noise ratio as the real neurons.

The receptive field sizes of both rod and horizontal cells were determined with a narrow slit of light ( $8 \mu\text{m} \times 750 \mu\text{m}$ ) flashed at various positions across the cell's receptive field (Lamb, 1976). The flash intensity was held constant and selected such

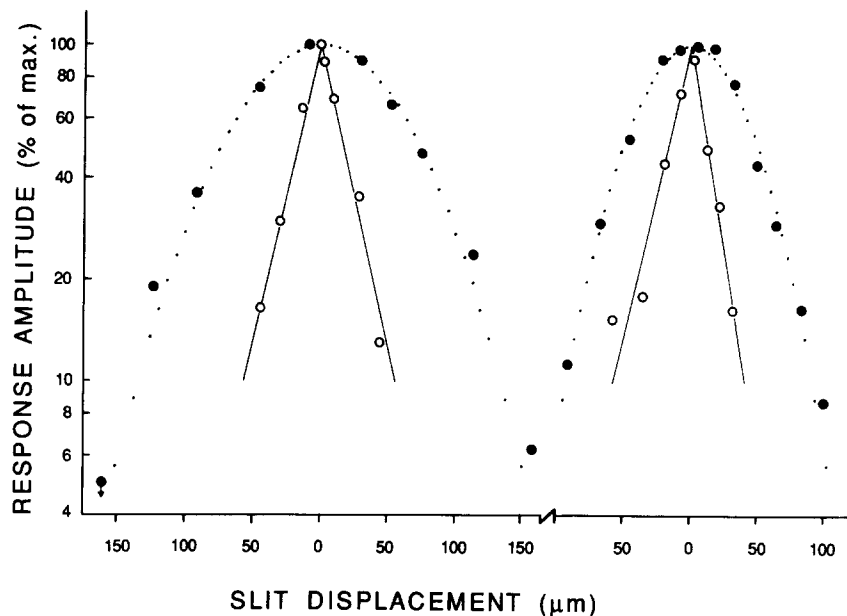


FIGURE 4. Receptive field of rods and horizontal cells. Peak response amplitudes to a flashed slit-shaped stimulus ( $8 \mu\text{m} \times 750 \mu\text{m}$ ) are plotted as function of slit displacement from the position of highest sensitivity in the receptive field of each cell. Open circles show rod response; filled circles horizontal cell responses. Straight lines are simple exponential decays having mean length constants of 24 and 22  $\mu\text{m}$  for the rods in the left and right panels, respectively. Dotted lines illustrate a Gaussian function with  $\sigma = 63 \mu\text{m}$  in the left and  $\sigma = 43 \mu\text{m}$  in the right panel.

that the maximum response was 1.5–3 mV. The rod data (Fig. 4, *open circles*) were satisfactorily fitted with straight lines when plotted on logarithmic ordinates, indicating that the peak response fell as a simple exponential of distance. The length constants ( $\lambda$ ) averaged 22.5  $\mu\text{m}$  ( $n = 8$ , see Table I) which is in good agreement with the results presented in previous studies (Leeper et al., 1978; Gold, 1979; Griff and Pinto, 1981). Receptive field profiles of two horizontal cells (Fig. 4, *filled circles*) reveal that these cells are driven by visual stimuli covering an area much larger than those of the rods. These and other horizontal cell data might have been fitted with functions having constant amplitude central plateaus (diameter, 20–100  $\mu\text{m}$ )



flanked by exponentially decreasing profiles. For seven cells, the exponential length constants that could be fitted to data at the flanks ranged from 27 to 61  $\mu\text{m}$  (Table I). As these length constants were significantly longer than those of rod receptive fields, we can conclude that electrical coupling between horizontal cells, in addition to rod-rod coupling, must contribute to the size of horizontal cell receptive fields.

Even though the exponential decays might be the most obvious mathematical representation for a network of electrically coupled cells, we have chosen to fit Gaussian functions to the horizontal cell receptive field data. This enabled us to determine, in a mathematically tractable way, a number of rods "representing" the receptive field (see below). The dotted lines in Fig. 4 plot the best-fitting two-dimensional Gaussian distributions. Table I lists the standard deviations ( $\sigma$ ) giving optimum fits to the horizontal cells investigated (mean = 50.7  $\mu\text{m}$ ), and the "representative radii"  $\sqrt{2} \sigma$ , i.e., the radii of cylinders having the same volumes and heights as the two-dimensional Gaussian "bodies" with standard deviations  $\sigma$  (see Appendix).

It should be noted that for four of seven horizontal cells it was found that the data farthest from the receptive field center lay clearly above the Gaussian curve drawn to fit the response amplitudes closer to the center (in no case did the data points lie significantly below the curve). Both this observation and data obtained with concentric circular stimuli of varying size suggest that the Gaussian model slightly underestimates the sensitivity of the far periphery, and thus also the size of the effective receptive field.

#### *Number of Rods "Representing" the Excitatory Receptive Fields of Horizontal Cells and Rods*

Using a circle of radius  $\sqrt{2} \sigma$  as the receptive field, and a rod density of 15,000  $\text{mm}^{-2}$  (Copenhagen et al., 1987), it was found that the mean number of rods enclosed in a horizontal cell receptive field is 250 (range, 91–373,  $n = 7$ ; see Table I).

In the case of rods, since the receptive field profiles were fitted by exponential and not Gaussian distributions, we needed to estimate the number of rods in a different but still comparable way. We could find no simple mathematical formulation to deduce this number. We have estimated the number by using analogies between the exponential rod receptive field and the two-dimensional Gaussian distribution describing the horizontal cell receptive fields. In the Gaussian distribution model, the events originating within the circle with the radius  $\sqrt{2} \sigma$  contribute 67% of the total response amplitude (full-field stimulus), and a slit stimulus tangential to this circle produces a relative response amplitude equal to 37% of the maximum response. We use these two figures as a base for estimating the rod receptive field. A calculation based on the response distribution for point stimuli (a modified Bessel function, see Lamb, 1976) shows that 67% of the total rod response stems from a circle with a radius = 1.76  $\lambda$ . On the other hand, a relative response amplitude of 0.37 is elicited by a slit at a distance of 1.00  $\lambda$  from the center. We used the mean of 1.00 and 1.76  $\lambda$ , i.e., 1.38  $\lambda$ , as the radius of a representative rod receptive field. A circle with this radius encompasses 55% of the total response to a full-field stimulus. If we correct for the contribution of scattered light to our measured  $\lambda$  value of 22.5

$\mu\text{m}$  (see Copenhagen and Owen, 1976; Gold, 1979) and take  $\lambda$  as  $20 \mu\text{m}$ , we get a radius of  $27.6 \mu\text{m}$  and a representative receptive field of 36 rods.

#### *Receptive Fields of Ganglion Cells*

A parallel study based on extracellular ganglion cell recordings indicated that the mean number of rods per ganglion cell receptive field was 1,950 (range, 740–4240,  $n = 7$ , Copenhagen et al., 1987). For all the calculations used to deduce the number of rods per receptive field we assume also that all cell types receiving rod inputs are connected to all red rods within their receptive fields. Considering the extensive rod-rod coupling, this seems a safe assumption.

#### *Receptive Field Sizes Derived from Response Variations*

On the assumption that the variability of responses is primarily photon-limited, it is possible to use the response amplitude fluctuations to estimate the number of rods contributing to the response of a retinal neuron. This approach was used to determine independently the number of rods per rod receptive field and per horizontal cell receptive field, respectively.

The calculations were based on the assumption that the number of isomerization events in each rod follows a Poisson distribution and that the events sum linearly. In line with our aim to define an imaginary group of equipotent rods (which can be said to represent the receptive field of a real cell), we made the simplifying assumption that each rod contributes to the response with signals of equal amplitude.

When  $N$  is the number of contributing rods and  $I$  is the flash intensity (in units  $\text{Rh}^*$ ) the product  $\mu_p = NI$  is a Poisson-distributed quantity and its standard deviation is  $\sigma_p = \sqrt{\mu_p}$ . Thus the average flash response is  $X = S_F I = (S_F/N)\mu_p$  and its standard deviation is  $\sigma = (S_F/N) \sqrt{\mu_p}$ . Using the ratio  $X/\sigma = \sqrt{\mu_p}$ , the number of contributing rods is:

$$N = (X/\sigma)^2 I^{-1} \quad (2)$$

Trains of flashes eliciting 1–1.6 mV (rods) or 1.7–3 mV (horizontal cells) responses were presented to the retina. It was possible to obtain data only in experiments having a minimum of low-frequency electrode and recording system noise (examples shown in Fig. 5). Response amplitude was measured as the difference between the voltage at the moment of the flash and the peak response. Data from seven rods and seven horizontal cells are given in Table II. The average numbers of contributing rods, 38 for rod and 255 for horizontal cell receptive fields, happen to be very close to the numbers 36 and 250 estimated from slit-determined receptive fields. Considering several sources of error (see below) the close agreement between the averages is somewhat fortuitous. As a way of judging the experimental precision, note that the horizontal cells 1–3 in Table II refer to the same cells as horizontal cells 1–3 in Table I. The response variability approach gave estimates that were 183, 75, and 157% of those obtained from the slit experiments.

The numbers of rods estimated in Table II would be decreased by possibly remaining low-frequency recording noise, and the intrinsic dark rod noise described by Baylor et al. (1980), since these are error sources that add to amplitude variability. On the other hand, the rod recordings used in Table II exceed the strictly linear intensity-response region (see Fig. 3). This again would tend to produce an overesti-

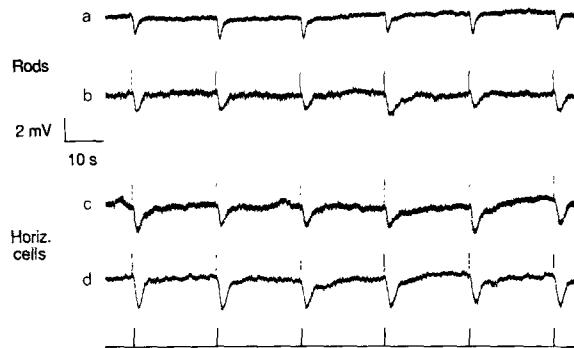


FIGURE 5. Intracellular recordings from two rods (*a, b*) and two horizontal cells (*c, d*). Flashes were given at 22-s intervals as indicated under the recordings. The upward "spikes" seen in the recordings and just preceding the flashes are pulses for 2-mV amplitude calibration. The four recordings shown were parts of the experiment presented in Table II; *a* and *b* correspond to rod

cells 1 and 2, and *c* and *d* to horizontal cells 6 and 7. Compared with rod *b*, rod *a* was less sensitive and less noisy, and its response had a much faster time course. The noise which is of interest here is seen as slow "bumps" lasting a few seconds. The high frequency noise which is especially evident in cells *b* and *c* is probably related to the recording technique and is thus of less interest. Analyzing just the series of six responses shown in this figure we find that the mean response amplitudes (and standard deviations) for cells *a, b, c,* and *d* are 1.52 (0.14), 1.50 (0.17), 1.80 (0.27), and 2.52 (0.19) mV. Considering the flash intensities given in Table II these data indicate receptive fields with 35, 51, 171, and 463 rods, respectively.

mation of the numbers of rods contributing to a rod receptive field. As both the slit method (see above) and the response variation tend to underestimate the number of rods in a horizontal cell receptive field we will use from now on the number 300 (instead of 250) for a "typical" horizontal cell.

## DISCUSSION

### *Causal Relation between Spatial Summation and Voltage Gain*

Both spatial summation and sensitivity increase by one order of magnitude as signals proceed from rods to horizontal cells, and by two orders of magnitude as they pro-

TABLE II  
*Number of Rods per Receptive Field Derived from Variance in Response Amplitude in Series of Responses to Weak Flashes with Fixed Mean Intensity*

Rods					Horizontal cells				
Cell	<i>n</i>	Rh*	<i>X/σ</i>	<i>N</i>	Cell	<i>n</i>	Rh*	<i>X/σ</i>	<i>N</i>
1	9	3.34	9.67	28	1	11	2.26	19.41	167
2	12	1.52	7.11	33	2	9	1.22	14.92	182
3	27	1.78	8.02	36	3	21	0.31	9.23	275
4	11	1.52	6.58	28	4	11	1.89	18.85	188
5	12	2.15	9.07	38	5	13	0.42	9.35	208
6	16	1.34	9.16	63	6	15	0.26	9.08	317
7	8	1.17	6.74	39	7	8	0.38	13.02	446
		Mean	Mean	38			Mean	Mean	255

*n* = number of responses in the series. The number of rods in the receptive field, *N*, was assumed to equal  $(X/\sigma)^2 \times I^{-1}$  where *X* stands for mean response amplitude, *σ* for standard deviation of response amplitude, and *I* for intensity (Rh\*). Observe that the value of *N* is significantly higher for horizontal cells even in cases when the flash intensities (Rh\*) and number of responses (*n*) used were very similar for both cell types.

ceed from rods to ganglion cells. These phenomena are clearly correlated; the large response amplification disappears if a horizontal or ganglion cell is stimulated by a small retinal spot corresponding to the receptive field of a single rod (see for instance Copenhagen et al., 1987, Fig. 1, the leftmost data point). Thus the signal stemming from one particular isomerization is not dramatically amplified. On the other hand there is no reason to expect the gain to be exactly one in a hypothetical synaptic transfer lacking spatial convergence. Thus we cannot quantitatively deduce the sensitivities of horizontal cells and ganglion cells from the rod sensitivity and the observed spatial convergence.

As we have measured only membrane potentials, but not resistance nor current, very little can be said about the synaptic mechanisms linking spatial summation and amplification. Here we just wish to point out that there is divergence as well as convergence in the actual retinal network. Counting nuclei in different retinal layers we have found that for each rod in the central *B. marinus* retina there are 0.7 cells in the ganglion cell layer and four to five second-order cells (bipolar and horizontal cells; we excluded most amacrine cells by not including the vitrealmost row of nuclei in the inner nuclear layer (Ramón y Cajal, 1972). Similar cell ratios have been found for the retina of the frog *Rana pipiens* (Maturana et al., 1960; Nilsson, 1964). Thus the channel convergence is balanced by a parallel divergence.

#### *Voltage Gain*

Dim flashes covering a substantial retinal area elicit responses of a larger amplitude at each subsequent level of processing in the retina. The average gain from rods to horizontal cells was roughly 7, that from rods to OFF bipolar cells very roughly 20, and from rods to ganglion cells often more than 100. Similar gains have been reported, before for the signal transmission through the toad retina (Belgum and Copenhagen, 1988), and for the retinas of the salamander (Capovilla et al., 1987), the turtle (Schnapf and Copenhagen, 1982; Baylor and Fettiplace, 1979), and the dogfish (Ashmore and Falk, 1980).

#### *Rod Hyperpolarization at Ganglion Cell Threshold*

Relating the mean rod sensitivity,  $0.9 \text{ mV/Rh}^*$ , to the ganglion cell thresholds ( $0.008\text{--}0.062 \text{ Rh}^*$  for stimuli covering the receptive field center; Copenhagen et al., 1987), we estimate that the hyperpolarization in the rod network needed for threshold responses in ganglion cells ranges from 7 to  $56 \mu\text{V}$ . This hyperpolarization is, of course, an average value summed over many rods, and our estimate neglects the stochastic nature of the placement of photons. One might argue that the important parameter for signal detection is not the response averaged from all rods but the few larger signals evoked in the individual rods by these dim stimuli. However, the extensive coupling between rods spreads the hyperpolarization to neighboring rods. Thus, the response in the rods "hit" by the photons would be on the order of  $10\text{--}100 \mu\text{V}$  due to coupling (Schwartz, 1975; Copenhagen and Owen, 1980).

The very small rod polarizations elicited at the dim light intensities corresponding to ganglion cell thresholds are certainly not unique. Calculations based on behaviorally determined increment thresholds and flash sensitivities of cones in the turtle suggest that a  $5\text{--}10\text{-}\mu\text{V}$  hyperpolarization in the cones is sufficient for reliable detec-

tion of light (Fain et al., 1977). In skate, *Raja clavata*, Brown and Govardovskii (1983) recorded activity of electroreceptors in Lorenzian ampullae and of axons innervated by these receptors. They demonstrated that reliable threshold responses in the axons corresponded to a 2–10- $\mu$ V polarization of the sensory cells.

#### *Ganglion Cells Driven from a Small Group of Rods*

From the results presented by Copenhagen et al. (1987, Fig. 1) it is evident that the rod hyperpolarizations must be much larger when small stimulus spots are used to produce threshold responses in ganglion cells. With spots covering only  $\sim 30$  rods, i.e., a small retinal area corresponding to one rod receptive field, they typically had to use 1–2 Rh\* flashes, i.e., 30–60 isomerizations, to produce ganglion cell responses, and it can be estimated that these flashes produce a hyperpolarization of 0.5–1.0 mV in the most central rods in this small retinal patch. Coincidentally, Baylor and Fettiplace (1977), recording from turtle ganglion cells while injecting current pulses into single rods, found that the current required for ganglion cell thresholds hyperpolarized the impaled rod by 1–2 mV.

#### *Receptive Fields Relevant to Signal-to-Noise Calculations*

The voltage gain in the signal transmission through the retina may clearly be one of the cellular mechanisms realizing a given response reliability at the ganglion cell level. But the ultimate limit of the response reliability, as defined by Eq. 1, is not a function of the gain, but of the spatial and temporal summations.

In the accompanying paper (Donner et al., 1990) we have determined the integration times of dark-adapted rods and horizontal cells; in this paper we have tried to define adequate receptive field sizes. The problem is that the receptive fields of horizontal and ganglion cells, and especially those of rods, have no obvious borders. Thus one may correctly conclude that a single rod is functionally coupled to thousands (Fain, 1976) or hundreds (Leeper et al., 1978) of other rods.

On the other hand, it is obvious that these numbers cannot correctly predict the reliability (signal-to-noise ratio) of a rod response. The random response variation must be dominated by a smaller group of rods which contribute with sizeable photon signals.

We have tried to solve the problem in a pragmatic way; for horizontal and ganglion cells we have used a top-hat receptive field model based on a two-dimensional Gaussian sensitivity distribution (see Appendix), and for rods we have used analogies between such a Gaussian distribution and the exponential rod receptive field. We propose that typical rod, horizontal cell, and ganglion cell receptive fields can be said to be represented by imaginary groups of 36, 300, and 2,000 equally effective and totally interconnected rods, in that such groups seem to predict the performance of these cell types in signal-to-noise discrimination (see Results for rods and horizontal cells; for ganglion cells see Aho et al., 1987; Copenhagen et al., 1987).

#### *Signal-to-Noise Ratios at Ganglion Cell Threshold*

The above rod numbers allow us to calculate maximum signal-to-noise ratios for rod, horizontal cell, and ganglion cell responses to a given flash stimulus covering the excitatory ganglion cell receptive field. The calculation is based on Eq. 1, on the

integration time 2 s for all three cell types (Donner et al., 1990), and the frequency 0.028 per rod and second for the spontaneous dark rod events at 20°C (Baylor et al., 1980; Copenhagen et al., 1987). For the flash intensity 0.03 Rh\*, which was found to be an average threshold among 19 dark-adapted ganglion cells (Copenhagen et al., 1987), we get the maximum signal-to-noise ratios 0.6, 1.8, and 4.6 for rods, horizontal cells, and ganglion cells, respectively.

The conclusion is that nonsignificant rod outputs can sum and drive reliable ganglion cell responses. The reason is that an increase in spatial summation by two orders of magnitude allows a one order of magnitude increase in reliability.

#### APPENDIX

##### *The Two-Dimensional Gaussian Function As a Model for the Sensitivity Distribution of Receptive Fields*

For purposes of comparison, we needed equivalent estimates for the number of rods encompassed by the receptive fields of horizontal and ganglion cells, respectively. Both ganglion and horizontal cell profiles were well fitted by Gaussian distributions. However, since ganglion cell receptive fields have usually been measured in the “top-hat” approximation, we shall here derive a “representative” radius that transforms the Gaussian distribution to a top-hat distribution comprised of a set of rods each having an equivalent effectiveness.

##### *The Representative Radius*

In circular coordinates, the relative sensitivity of a two-dimensional Gaussian function at a radius  $r$  is:

$$z = z_0 e^{-r^2/2\sigma^2} \quad (\text{A1})$$

where  $z_0$  is the sensitivity at the origin,  $r = 0$ . The integral sensitivity is the volume of the rotational body under the surface  $z(r)$ :

$$\int_0^\infty z(r) 2\pi r dr = 2\pi\sigma^2 z_0 \quad (\text{A2})$$

If one replaces this Gaussian by a representative cylindrical (top-hat) distribution of the same peak sensitivity  $z_0$  and the same total sensitivity (i.e., volume), then:

$$\pi R_c^2 z_0 = 2\pi\sigma^2 z_0 \quad (\text{A3})$$

where  $R_c = \sqrt{2}\sigma$  and is the representative radius. Thus a cylinder of radius  $R_c = \sqrt{2}\sigma$  will have the same volume as a two-dimensional Gaussian function of the same height and standard deviation  $\sigma$ . The number of equally effective rods in the top-hat receptive field is then  $\pi R_c^2 D$  where  $D$  is the density of rods (number/mm<sup>2</sup>).

##### *Determination of $\sigma$ Using Slit-shaped Stimuli*

Circular and slit-shaped stimuli were used to measure ganglion and horizontal cell receptive fields, respectively. The derivation below demonstrates that sensitivity profiles obtained with the slit have the same  $\sigma$  as the underlying Gaussian function. On rectangular coordinates, assume that the slit of width  $dy$ , is parallel to the  $x$ -axis and is placed at  $y_1$ . The sensitivity of the response to the slit is proportional to the volume  $dV$  sliced from the two-dimensional Gaussian function:

$$dV = dy \int_{-\infty}^{\infty} z dx = z_0 dy \int_{-\infty}^{\infty} e^{-(x^2 + y_1^2)/2\sigma^2} dx \quad (\text{A4})$$

$$dV = z_0 dy e^{-y^2/2\sigma^2} \int_{-\infty}^{\infty} e^{-x^2/2\sigma^2} dx \quad (\text{A5})$$

$$dV = dV_{\max} e^{-y^2/2\sigma^2} \quad (\text{A6})$$

where  $dV_{\max}$  is the peak sensitivity for the slit positioned at the center of the field ( $y_1 = 0$ ). As the slit is moved along the  $y$ -axis, the observed sensitivity changes as  $\exp(-y^2/2\sigma^2)$ .

We wish to thank Drs. J. Ashmore, W. G. Owen and D. A. Baylor for the helpful comments on earlier versions of the manuscript. We are grateful for the discussions and valuable insights provided by Drs. Kristian Donner and Jack Belgum.

This study was supported by National Institutes of Health EY-01869 (D. R. Copenhagen) and by the Academy of Finland (S. Hemilä and T. Reuter). Dr. Reuter was a recipient of an ASLA-Fulbright travel and research grant and a Research to Prevent Blindness Travel Award.

*Original version received 4 November 1988 and accepted version received 7 June 1989.*

#### REFERENCES

- Aho, A.-C., K. Donner, C. Hydén, T. Reuter, and O. Y. Orlov. 1987. Retinal noise, the performance of retinal ganglion cells, and visual sensitivity in the dark-adapted frog. *Journal of the Optical Society of America A*. 4:2321–2329.
- Ashmore, J. F., and D. R. Copenhagen. 1983. An analysis of transmission from cones to hyperpolarizing bipolar cells in the retina of the turtle. *Journal of Physiology*. 340:569–597.
- Ashmore, J. F., and G. Falk. 1980. Responses of rod bipolar cells in the dark-adapted retina of the dogfish, *Scyliorhinus canicula*. *Journal of Physiology*. 300:115–150.
- Attwell, D., S. Borges, S. M. Wu, and M. Wilson. 1987. Signal clipping by the rod output synapse. *Nature*. 328:522–524.
- Barlow, H. B. 1964. The physical limits of visual discrimination. In *Photophysiology*. Vol. 2. A. C. Giese, editor. Academic Press, New York. 163–202.
- Baylor, D. A., and R. Fettiplace. 1977. Transmission from photoreceptors to ganglion cells in the retina of the turtle. In *Vertebrate Photoreception*. H. B. Barlow and P. Fatt, editors. Academic Press, London. 193–203.
- Baylor, D. A., and R. Fettiplace. 1979. Synaptic drive and impulse generation in ganglion cells of turtle retina. *Journal of Physiology*. 288:107–127.
- Baylor, D. A., G. Matthews, and K.-W. Yau. 1980. Two components of electrical dark noise in toad retinal rod outer segments. *Journal of Physiology*. 309:591–621.
- Belgum, J. H., and D. R. Copenhagen. 1988. Synaptic transfer of rod signals to horizontal and bipolar cells in the retina of the toad (*Bufo marinus*). *Journal of Physiology*. 396:225–245.
- Belgum, J. H., D. R. Copenhagen, and T. Reuter. 1983. The missing “nose”: kinetics of transfer across the rod-horizontal cell synapse in *Bufo* retina. *Investigative Ophthalmology and Visual Science*. 24(Suppl.):179. (Abstr.)
- Brown, G. R., and V. I. Govardovskii. 1983. Receptor mechanisms of the Lorenzian ampullae electroreceptors in skates. *Neirofiziologiya*. 15:178–185.
- Brown, J. E., and L. H. Pinto. 1974. Ionic mechanism for the photoreceptor potential of the retina of *Bufo marinus*. *Journal of Physiology*. 236:575–591.
- Brown, K. T., and D. G. Flaming. 1977. New microelectrode techniques for intracellular work in small cells. *Neuroscience*. 2:813–827.
- Capovilla, M., M. A. Hare, and W. G. Owen. 1987. Voltage gain of signal transfer from retinal rods to bipolar cells in the tiger salamander. *Journal of Physiology*. 391:125–140.

- Copenhagen, D. R., K. Donner, and T. Reuter. 1987. Ganglion cell performance at absolute threshold in toad retina; effects of dark events in rods. *Journal of Physiology*. 393:667–680.
- Copenhagen, D. R., and W. G. Owen. 1976. Functional characteristics of lateral interactions between rods in the retina of the snapping turtle. *Journal of Physiology*. 259:251–282.
- Copenhagen, D. R., and W. G. Owen. 1980. Current-voltage relations in the rod photoreceptor network of the turtle retina. *Journal of Physiology*. 308:159–184.
- Donner, K. 1981. Receptive fields of frog retinal ganglion cells: response formation and light-dark adaptation. *Journal of Physiology*. 319:131–142.
- Donner, K. 1989. The absolute sensitivity of vision: can a frog become a perfect detector of light-induced and dark rod events? *Physica Scripta*. 39:133–140.
- Donner, K., D. R. Copenhagen, and T. Reuter. 1990. Weber and noise adaptation in the retina of the toad, *Bufo marinus*. *Journal of General Physiology*. 95:733–753.
- Fain, G. L. 1975. Quantum sensitivity of rods in the toad retina. *Science*. 187:838–841.
- Fain, G. L. 1976. Sensitivity of toad rods: dependence on wavelength and background illumination. *Journal of Physiology*. 261:71–101.
- Fain, G. L., A. M. Granda, and J. H. Maxwell. 1977. Voltage signal of photoreceptors at visual threshold. *Nature*. 265:181–183.
- Gold, G. H. 1979. Photoreceptor coupling in retina of the toad, *Bufo marinus*. II. Physiology. *Journal of Neurophysiology*. 42:311–328.
- Griff, E. R., and L. H. Pinto. 1981. Interactions among rods in the isolated retina of *Bufo marinus*. *Journal of Physiology*. 314:237–254.
- Hassin, G., and P. Witkovsky. 1983. Intracellular recording from identified photoreceptors and horizontal cells of the *Xenopus* retina. *Vision Research*. 23:921–931.
- Lamb, T. D. 1976. Spatial properties of horizontal cell responses in the turtle retina. *Journal of Physiology*. 263:239–255.
- Leeper, H. F., R. A. Normann, and D. R. Copenhagen. 1978. Evidence for passive electronic interactions in red rods of toad retina. *Nature*. 275:234–236.
- Maturana, H. R., J. Y. Lettvin, W. S. McCulloch, and W. H. Pitts. 1960. Anatomy and physiology of vision in the frog (*Rana pipiens*). *Journal of General Physiology*. 43:129–175.
- Nilsson, S. E. G. 1964. Interreceptor contacts in the retina of the frog (*Rana pipiens*). *Journal of Ultrastructure Research*. 11:147–165.
- Ogden, T. E., G. G. Mascetti, and R. Pierantoni. 1984. The internal horizontal cell of the frog: analysis of receptor input. *Investigative Ophthalmology and Visual Science*. 25:1382–1394.
- Ramón y Cajal, S. 1972. *The Structure of the Retina*. Thomas, Springfield, IL. 196 pp.
- Reuter, T., K. Donner, and D. R. Copenhagen. 1986. Does the random distribution of discrete photoreceptor events limit the sensitivity of the retina? *Neuroscience Research*. 4:(Suppl.)S163–S180.
- Schnapf, J. L., and D. R. Copenhagen. 1982. Differences in the kinetics of rod and cone synaptic transmission. *Nature*. 296:862–864.
- Schwartz, E. A. 1975. Rod-rod interaction in the retina of the turtle. *Journal of Physiology*. 246:617–638.